

Spectroscopic Study of Rh^{105} by Direct (He^3, d) and (p, α) Reactions*

D. L. Dittmer† and W. W. Daehnick

Nuclear Physics Laboratory, University of Pittsburgh, Pittsburgh, Pennsylvania 15213

(Received 6 February 1970)

The level structure of ${}_{45}\text{Rh}^{105}$, below 2 MeV in excitation, was studied by $\text{Ru}^{104}(\text{He}^3, d)\text{Rh}^{105}$ at $E_{\text{He}^3} = 18$ MeV, and by $\text{Pd}^{108}(p, \alpha)\text{Rh}^{105}$ at $E_p = 15$ MeV. An Enge split-pole spectrograph was used for high-resolution analysis of the reaction products. Particle detection for deuterons was achieved with nuclear emulsions, while position-sensitive "triode" counters were used for the α particles. Targets were kept thin enough to permit total experimental resolutions of 12–13 keV. Comparison of 17 measured (He^3, d) angular distributions with nonlocal, finite-range distorted-wave Born-approximation (DWBA) calculations indicated a predominance of $l=2$ transfers, and yielded J^π limits for the more strongly excited states. Differential $\text{Pd}^{108}(p, \alpha)\text{Rh}^{105}$ cross sections were obtained over the angular range of from 8 to 100° and complement the (He^3, d) measurements, frequently exciting levels not seen in proton stripping. DWBA triton-cluster transfer calculations reproduce the empirically observed $l=1$ j dependence. A weaker, but detectable, j dependence is predicted for $l=3$. The observed Rh^{105} energy-level scheme is compared with weak-coupling-model expectations and the results of earlier β -decay studies.

I. INTRODUCTION

Previous high-resolution studies with direct transfer reactions in the Pd region¹ have added considerably to the understanding of these nuclei. We have found it particularly interesting that the j dependence for $l=1$ in direct (p, α) ¹ and (α, p) ² reactions can be well reproduced by distorted-wave Born-approximation (DWBA) calculations, and thus become a significant aid in the spectroscopy of odd- A nuclei. The study of Rh^{105} aims at further insight in the level structure of nuclei in this vibrational region. It was hoped and found true that the (p, α) transitions would supplement the (He^3, d) measurements, and possibly also reveal j dependence for higher l transfers.

Initially, Rh^{105} had been studied exclusively through β decay of Ru^{105} , which resulted in an incomplete and somewhat uncertain level scheme for this nucleus.^{3–7} Recent high-resolution β - γ and γ - γ work⁸ has cleared up many earlier inconsistencies but, owing to the selectivity involved in radioactive decay, still has not led to a complete nuclear energy-level diagram. The triton pickup and proton stripping investigations undertaken here complement the decay studies and further extend the spectroscopy of Rh^{105} to 2 MeV in excitation.

II. EXPERIMENTAL METHOD

A. $\text{Ru}^{104}(\text{He}^3, d)\text{Rh}^{105}$

This proton stripping study was undertaken at a He^3 bombarding energy of 18 MeV, and particle analysis was performed using our Enge split-pole

spectrograph and photographic emulsions. Emerging deuterons were detected over an angular range from 10 to 45° .

The experiment marked the initial use of our (High Voltage Engineering Corporation D-EN-SO-66) helium-ion source, and considerable difficulty in obtaining ion beams of usable magnitude was experienced during the early stages of operation. The negative injection system, incorporating Li-vapor charge exchange, initially yielded beam currents typically about an order of magnitude less than the 4- μA specified output. Subsequent source development included alignment, source-box vacuum improvement, reduction of extractor electrode loading, and optimization of source operating parameters, and led to a much improved (2- to 3- μA) negative helium beam. This output produced 0.2 to 0.3 μA on target through a 3-mm-high by 1-mm-wide beam-defining slit, which was a marginally acceptable current for the single-nucleon transfer (He^3, d) experiment.

B. $\text{Pd}^{108}(p, \alpha)\text{Rh}^{105}$

Differential (p, α) cross sections were obtained over the angular range from 8 to 100° at an incident proton energy of 15 MeV. The multiple Si-surface-barrier-detector arrangement employed previously¹ for all but forward-angle $\text{Ag}(p, \alpha)$ measurements did not offer sufficient resolution to be useful for the high-level density experienced in the residual odd- A Rh^{105} . In addition, the energetics of the competing (p, d) and (p, t) reactions were such that conventional magnetic analysis using nuclear emulsions would not provide adequate α -particle discrimination. Consequent-

ly, the $Pd^{108}(p, \alpha)$ experiment required the use of position-sensitive counters placed in the focal plane of the spectrograph to satisfy the particle-identification and high-resolution requirements. Four position-sensitive "silicon triode" counters spanned a total distance of about 200 mm along the focal plane. The detectors, having depletion depths of 450 to 600 μ , were each 40 to 50 mm in sensitive length. Two spectrograph field settings per angle were necessary in order to bridge the gaps between counters and achieve a continuous energy spectrum.

C. Spectra and Resolution

Figure 1 exhibits a deuteron spectrum for $Ru^{104}(\text{He}^3, d)Rh^{105}$ taken at $\theta = 20^\circ$. Light impurity groups corresponding to the $C^{13}(\text{He}^3, d)N^{14}$ and the $N^{14}(\text{He}^3, d)O^{15}$ ground-state reactions were identi-

fied by their systematic displacement with angle.

Within the limited peak definition imposed by low counting statistics, single-state widths measure about 0.7 mm or 13 keV for 19-MeV particles. An estimate of the contributions to the resolution was performed as outlined in Ref. 1, and the results for the (He^3, d) study are listed in Table I. Low target currents dictated the use of larger-than-optimum source size and horizontal-divergence-limiting slits, and major linewidth-broadening contributions arose from items (a) and (b).

A typical $Pd^{108}(p, \alpha)$ energy spectrum, obtained by combining information from several position-sensitive detectors, is shown in Fig. 2. Differential cross sections for the 25° run displayed are 90 $\mu\text{b}/\text{sr}$ for the 0.150-MeV level and 25 $\mu\text{b}/\text{sr}$ for the first excited state at 0.129 MeV.

The excellent experimental resolution of 12 keV, about one half that obtained in the earlier $Ag(p, \alpha)$ investigations,¹ resulted primarily from the use of

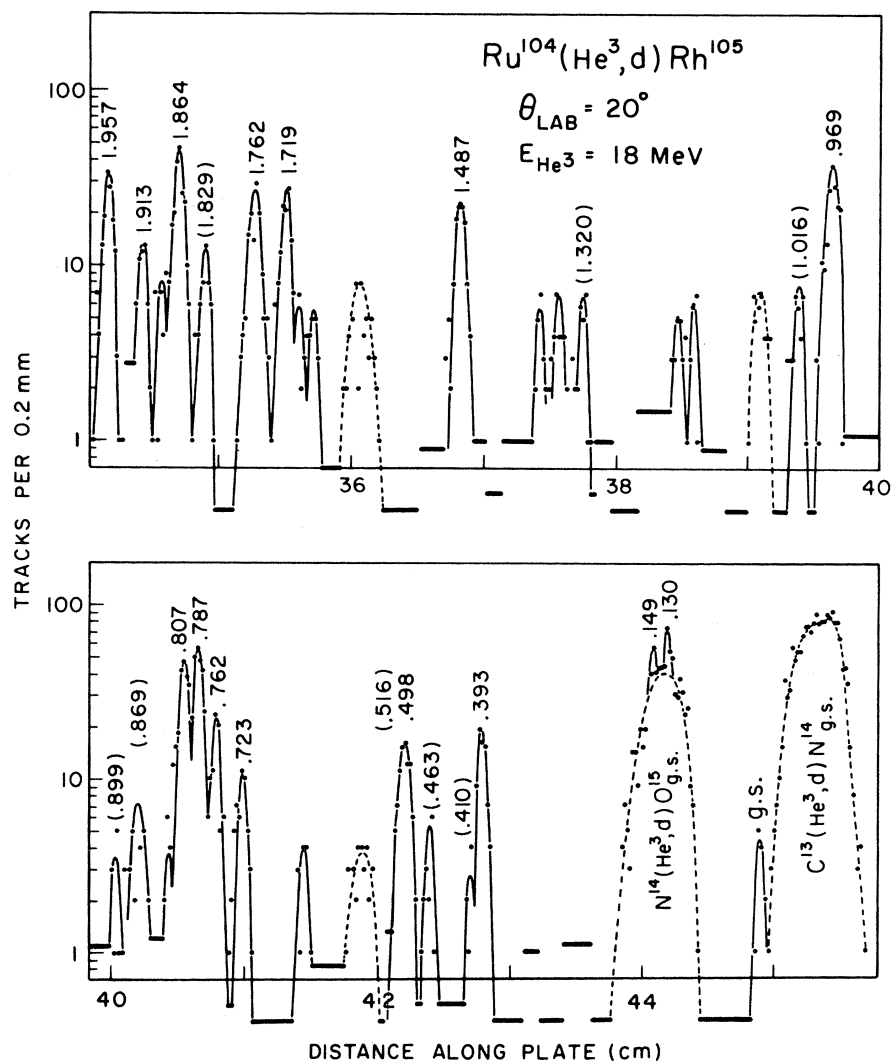


FIG. 1. Spectrum of levels in Rh^{105} populated by $Ru^{104}(\text{He}^3, d)Rh^{105}$ at a bombarding energy of 18 MeV. Resolution is of the order of 13 keV for 19-MeV deuterons.

TABLE I. Calculated contributions to the experimental resolution for 19-MeV deuterons and 18-MeV α particles from the $\text{Ru}^{104}(\text{He}^3, d)\text{Rh}^{105}$ and $\text{Pd}^{108}(p, \alpha)\text{Rh}^{105}$ reactions (see Figs. 1 and 2). Energies are in keV.

	$\text{Ru}^{104}(\text{He}^3, d)$ $\theta = 20^\circ$	$\text{Pd}^{108}(p, \alpha)$ $\theta = 25^\circ$
(a) Source size $\frac{1}{2} \frac{\cos \theta - \alpha }{\cos \alpha}$ (mm)	$\lesssim 10.0$	$\lesssim 10.5$
(b) Kinematic broadening due to horizontal divergence of the incident beam	$\lesssim 7.0$	$\lesssim 6.5$
(c) Increase in source size due to divergence between slit and target	$\lesssim 3.0$	$\lesssim 2.5$
(d) Target thickness, straggling, and differential loss	3.0	4.5
(e) Spectrograph aberration	4.0	3.5
(f) Incident beam energy spread	~ 3.0	~ 2.0
(g) Plate scanning resolution	4.0	
(h) Position-counter resolution		~ 7.0
(i) Miscellaneous factors including spectrograph and analyzing-magnet field fluctuations and incorrect focal-plane positioning	~ 2.0	~ 2.0
Total calculated resolutions $(\sum_i \epsilon_i^2)^{1/2}$	$\lesssim 14.6$	$\lesssim 15.8$

targets an order of magnitude thinner than those employed in the Ag work. Calculated contributions to the resolution are listed in the second column of Table I. In view of the small amount of spectrograph target-slit current (less than 10% of the on-target beam), the sizable calculated linewidth due to source size and horizontal divergence can be

regarded as upper limits, and a realistic reduction of these items would yield a calculated resolution more in agreement with the actual measured value. The counter spatial resolution, stated at <1% of the detector length,⁹ was estimated to be 0.4 mm, and contributed about $\lesssim 7$ -keV broadening.

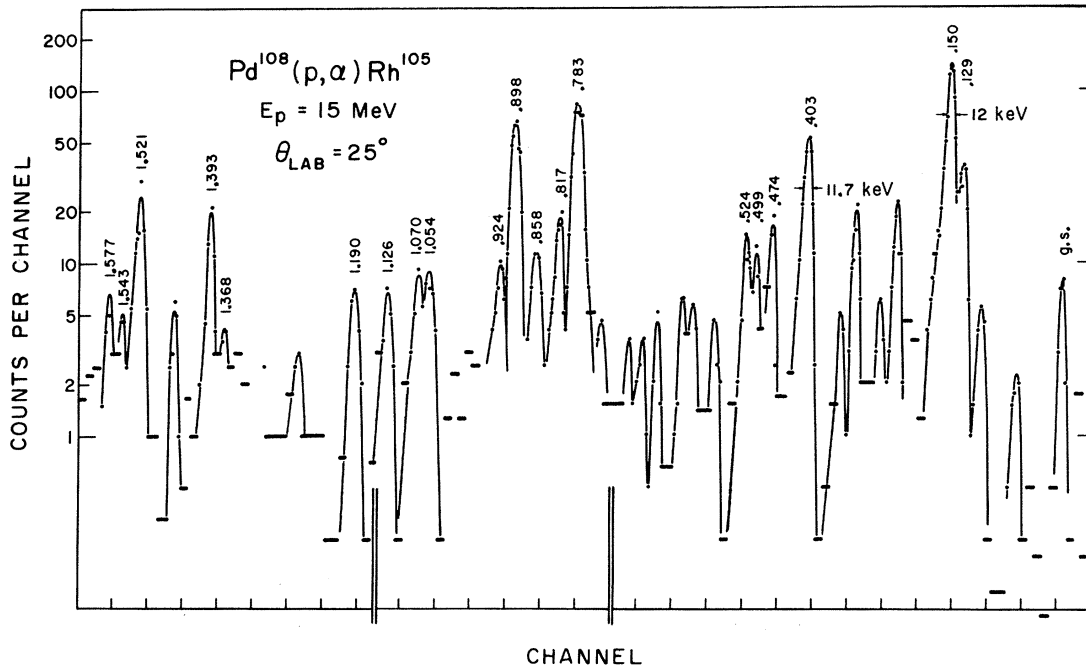


FIG. 2. $\text{Pd}^{108}(p, \alpha)\text{Rh}^{105}$ energy spectrum obtained by piecing together information from three position-sensitive counters. 12-keV resolution was achieved by using targets an order of magnitude thinner than those employed in the earlier Ag(p, α) work. (See Ref. 1.)

Targets of Ru¹⁰⁴ and Pd¹⁰⁸ were prepared on 20–30- $\mu\text{g}/\text{cm}^2$ carbon backings by electron-gun bombardment of metallic powders of 99.7 and 94.2% isotopic enrichment, respectively. Difficulty was encountered in maintaining the Ru metal, because of its high melting point, at a sufficient vaporization temperature without damaging the carbon foil; and thinner than desired Ru¹⁰⁴ deposits, 20–25 $\mu\text{g}/\text{cm}^2$, resulted. The Pd¹⁰⁸ target, 25 $\mu\text{g}/\text{cm}^2$ thick, contained roughly 20% Ta impurity derived from the boat material.

D. Experimental Errors

As standard procedure, differential-cross-section uncertainties associated with counting statistics, background subtraction, particle-group separation, and charge- to monitor-ratio fluctuations were treated as random errors and indicated by error bars drawn through the experimental data points.

The Ru¹⁰⁴ target thickness was determined by He³ elastic scattering in comparison with known Pd targets, and a $\pm 12\%$ scale error was estimated for the Ru¹⁰⁴ thickness. Three independent Pd¹⁰⁸ target-thickness measurements produced agreement to better than $\pm 6\%$, and an absolute error of this magnitude was assigned to this more precise determination.

Other scale uncertainties associated with the (He³, d) experiment include charge-collection normalization (better than $\pm 8\%$), absolute uncertainty of the spectrograph acceptance solid angle ($\sim \pm 5\%$), and plate scanning inconsistencies (observed to be within $\pm 10\%$ for this work). The latter error, of course, does not affect the Pd¹⁰⁸(p , α) position-sensitive counter data. In addition, comparison of spectrograph runs in the (p , α) work to results of surface-barrier-detector experiments essentially eliminated any sizable solid-angle uncertainty. Charge collection was believed to be uncertain to less than $\pm 5\%$ for the (p , α) studies. Based on the above estimates, a scale error of ± 20 – 25% is assigned to the (He³, d) data, and an absolute un-

certainty of less than $\pm 15\%$ is estimated for the (p , α) results.

Excitation energies for levels in Rh¹⁰⁵ could be determined with a systematic error of about 1% from the (He³, d) spectra using the energies computed by the code SPECTRE.¹⁰ These values were then recalibrated to well-known levels measured in the high-resolution Ru¹⁰⁵ decay study of Schriber and Johns,⁸ with the result that our final assignments are estimated to be accurate within $\pm 0.25\%$. The nonlinear response of position-sensitive counters made (p , α) absolute level assignments more difficult. Energy calibration of the entire system was achieved with elastically scattered deuterons as described in the work of Daehnick.¹¹ Excitation energies obtained from this (p , α) experiment are believed to be typically uncertain by ± 5 keV.

III. DISTORTED-WAVE ANALYSIS AND EXPERIMENTAL RESULTS

A. Ru¹⁰⁴(He³, d)Rh¹⁰⁵

Theoretical calculations were carried out using the DWBA code DWUCK¹² and included the use of both a zero-range, local option and a finite-range, nonlocal option. Optical-model parameters for the entrance channel were obtained from He³ elastic scattering on Zr⁹⁴ by Rundquist, Brussel, and Yavin,¹³ and deuteron channel parameters were the same as those used in the Pd¹⁰⁵(d , t) and Pd¹⁰⁵(d , p) analyses.¹ The bound-state proton well was described by the geometry $r_0 = r_c = 1.25$ F, $a = 0.65$ F, and $\lambda_{s_0} = 25$; identical to the values employed in the neutron transfer calculations. Nonlocality correction factors $\beta_{\text{He}^3} = 0.3$ (suggested by Parkinson *et al.*¹⁴) and $\beta_d = 0.54$, and a finite-range parameter¹² $R = 0.77$ were used. In Table II are listed the parameters that enter in the DWBA calculations.

The Ru¹⁰⁴ target contains 16 protons in the $N = 28$ to 50 shell, and stripping is expected to lead to the single-particle orbits within this shell as well as to the low-lying $1g_{7/2}$ and $2d$ levels of the next

TABLE II. Optical-model parameters and bound-state well geometries employed in the Ru¹⁰⁴(He³, d)Rh¹⁰⁵ and Pd¹⁰⁸(p , α)Rh¹⁰⁵ distorted-wave calculations.

Channel	V_S (MeV)	r_{0S} (F)	r_{0C} (F)	a_S (F)	W_S (MeV)	$4W_D$ (MeV)	r_{0I} (F)	a_I (F)	V_{s_0} (MeV)	β (F)	R (F)
Ru(He ³ , He ³)	176.4	1.14	1.4	0.71	14.5	...	1.54	0.78	...	0.3	...
Rh(d , d)	103	1.09	1.09	0.85	...	49.6	1.41	0.90	...	0.54	...
Pd(p , p)	51.56	1.25	1.25	0.65	...	65.08	1.25	0.47	7.5
Rh(α , α)	150	1.49	1.49	0.60	20	...	1.49	0.60
proton well	...	1.25	1.25	0.65	$\lambda = 25$...	0.770
triton well	...	1.38	1.38	0.45	$\lambda = 25$

higher shell. Figure 3 presents distorted-wave calculations for anticipated proton transfers in $\text{Ru}^{104}(\text{He}^3, d)\text{Rh}^{105}$. The two sets of curves represent finite-range, nonlocal potential (solid), and zero-range, local (dashed) predictions. The former corrections increase the magnitude of the bound-state wave-function tail and lead to an enhancement in cross section at the stripping peak of about 12% for p, d and g transfer, and 18% for the $f_{5/2}$ calculation. A slight displacement toward larger angles is noted for the first maximum in the finite-range, nonlocality pattern, particularly for the $f_{5/2}$ prediction. Little discernible change in shape was noted by the inclusion of $\vec{l} \cdot \vec{\sigma}$ coupling in the form factor, although the magnitude increase for the $j=l+\frac{1}{2}$ calculations with respect to the $j=l$ predictions was 5% for $p_{3/2}$, 9% for $d_{5/2}$, and 32% for $g_{9/2}$.

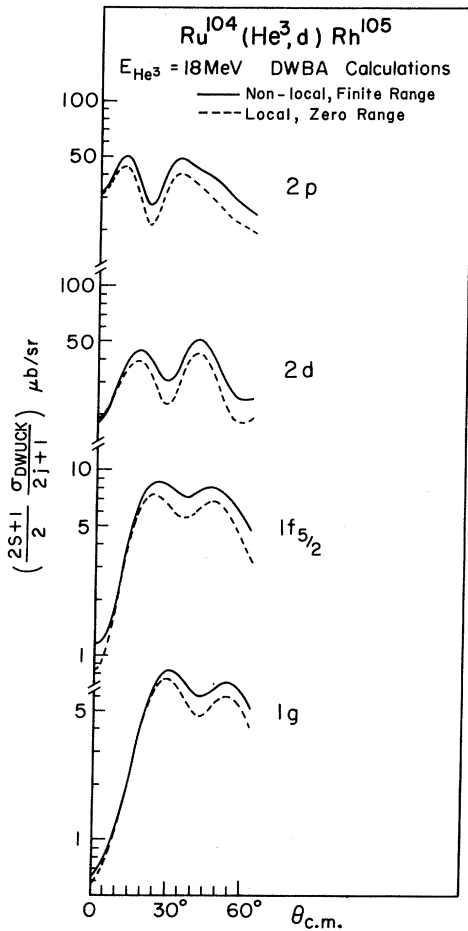


FIG. 3. DWBA calculations for anticipated proton transfers in $\text{Ru}^{104}(\text{He}^3, d)\text{Rh}^{105}$ at 18 MeV. "Nonlocal, finite-range" corrections increase the magnitude of the bound-state wave-function tail and lead to an enhancement in the predicted cross section.

Experimental angular distributions to levels more strongly excited in the $\text{Ru}^{104}(\text{He}^3, d)\text{Rh}^{105}$ study are displayed in Fig. 4. DWBA predictions that best reproduce the data for each of the observed transitions are indicated.

For a 0^+ target the spin and parity of the state in the residual nucleus are identical to the J^π of the stripped proton; and l_j mixing that complicated the Pd^{104} and Pd^{106} analyses¹ was absent. However, in some cases large statistical errors and relatively structureless angular distributions made the l assignment ambiguous, and l determinations for several of the transitions must be regarded as tentative, as indicated.

Table III lists the excitation energies, l values, J^π limits, differential cross sections measured at the stripping peak, and spectroscopic strengths $(2I_f+1)S$ for levels in Rh^{105} excited by (He^3, d) and by (p, α) . In addition, assignments derived from the most complete previous study of this nucleus, the Ru^{105} decay investigations of Schriber and Johns,⁸ are included along with suggested J^π designations based on the total available spectroscopic information.

With Bassel's¹⁵ normalization (neglecting the Coulomb interaction in the proton-deuteron system) the (He^3, d) differential cross section for an even-even target is expressed as

$$\left(\frac{d\sigma}{d\Omega}\right)_{\text{exp}} = 4.42(2I_f+1)S \left(\frac{2s+1}{2} \frac{\sigma_{\text{DWUCK}}(\theta)}{2j+1}\right). \quad (1)$$

Here, $I_f=j$, the total angular momentum of the transferred particle; S is the spectroscopic factor, and the remaining term in parentheses represents the calculated cross section (Fig. 3).

Defining

$$(2I_f+1)S=S', \quad (2)$$

and summing over all states k described by a given single-particle transfer, one obtains (following Yoshida¹⁶)

$$\sum_k S'_k = (2j+1)U_j^2 = (2j+1)-n, \quad (3)$$

where n equals the number of protons in the shell-model state j . Thus the summed strength yields directly the number of holes in this orbital.

The uncertainty in l transfer assignments for $l=2$ and 3, and the limited region of excitation covered do not permit us to deduce absolute l_j occupancies from the summed spectroscopic factors. However, surprisingly many of the transitions seem to be fairly well reproduced by $1f_{5/2}$ calculations. Only one transition, to the 0.149-MeV second excited state, displayed any marked $l=4$ strength. Since stripping is likely to both $I_f=l\pm\frac{1}{2}$

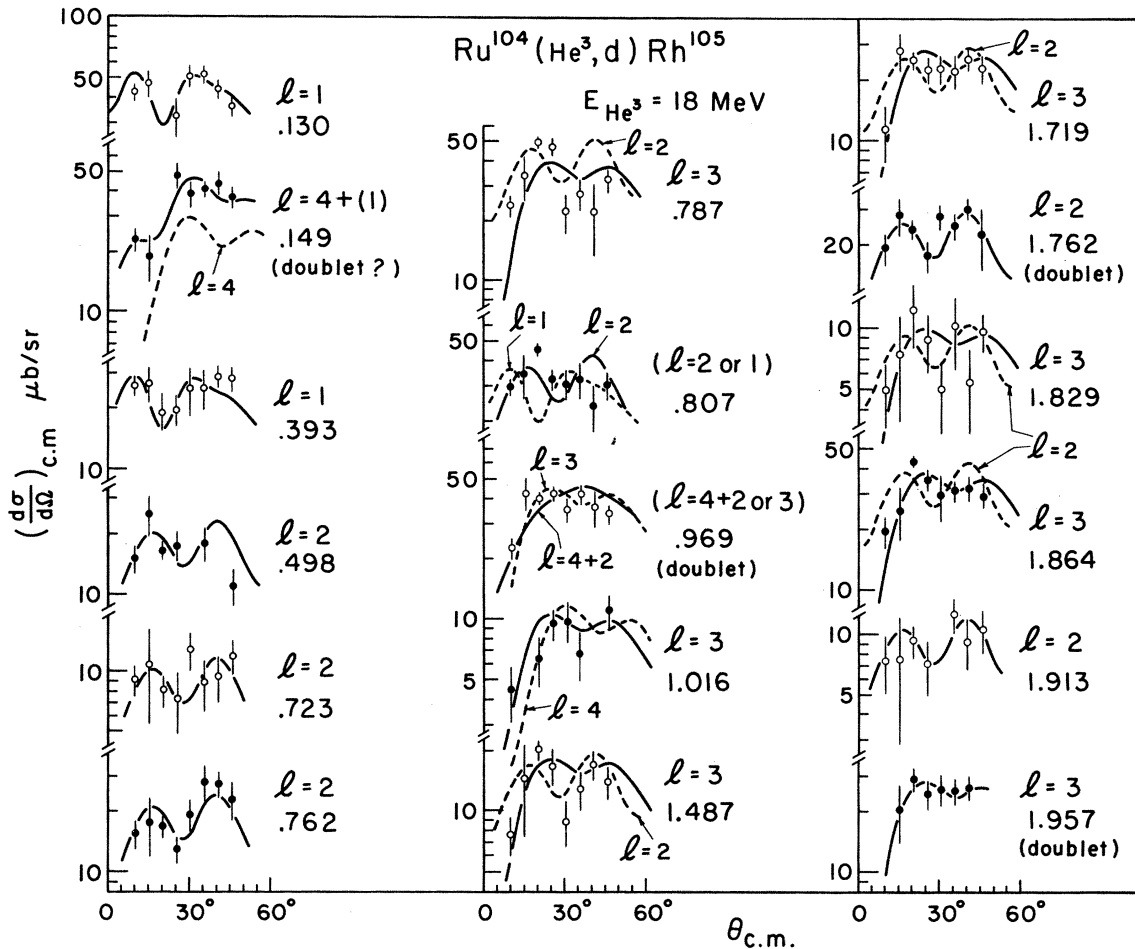


FIG. 4. $Ru^{104}(He^3, d)Rh^{105}$ experimental angular distributions in comparison with "nonlocal, finite-range" DWBA predictions (curves). Large statistical errors and relatively structureless angular distributions often make l assignments ambiguous.

levels for p , d and g transfer, the spectroscopic strengths extracted for these transitions are based on spin-independent calculations.

B. $Pd^{108}(p, \alpha)Rh^{105}$

The (p, α) DWBA calculations were performed with the same zero-range, macroscopic-model assumptions as those employed in our $Ag(p, \alpha)$ work.¹ Woods-Saxon-well optical parameters were from the same families^{17,18} as used in these earlier calculations, and are listed, along with the triton bound-state potential geometry, in Table II.

Whereas the $\frac{1}{2}^-$ - Ag -target spins allowed l_j mixtures for transitions to other than 0^+ final states, the even-even Pd^{108} target dictates that the spin and parity of levels in the residual nucleus be uniquely determined by the quantum numbers of the picked-up triton. Shown along the left side of

Fig. 5 are transfers described as $l=1$. A j dependence is noted in comparing the experimental angular distributions for the known 0.129-MeV ($\frac{1}{2}^-$) and 0.783-MeV ($\frac{3}{2}^-$) levels, and is well reproduced by the calculated curves. A significant, but less distinctive j effect was predicted for the $l=3$ DWBA calculations (see Fig. 6). However, the lack of well-known $\frac{5}{2}^-$ and $\frac{7}{2}^-$ Rh^{105} levels, as well as sizable statistical errors associated with the large-angle data, rendered experimental verification of j dependence for f transfer uncertain.

On the right of Fig. 5 are displayed data best duplicated by $f_{7/2}$ and $g_{9/2}$ predictions. The forward-angle enhancement noted for pickup to the known $\frac{9}{2}^+$ second excited state could be indicative of the presence of an $l=1$ transition, and may suggest a doublet assignment for this level. In Fig. 6 are shown angular distributions of less-pronounced structure to more weakly excited levels in Rh^{105} . Several calculated curves for each of

TABLE III. Experimental results for levels in Rh^{105} excited by $Ru^{104}(He^3, d)Rh^{105}$ and $Pd^{108}(p, \alpha)Rh^{105}$, and a comparison with Ru^{105} decay studies (see Ref. 8).

Excitation energy (MeV)	Ru ¹⁰⁴ (He ³ , d)Rh ¹⁰⁵			Pd ¹⁰⁸ (p, α)Rh ¹⁰⁵			β-γ decay ^b			Suggested J ^π assignment
	l	$\frac{d\Omega}{d\sigma}$ (μb/sr)	(2f + 1)S	Excitation energy (MeV)	L_j	(dσ/dΩ) _{max} (μb/sr)	J ^π limits present work	Excitation energy (MeV)	J ^π	
0	...	(≤1μb/sr)	...	0	...	very weak	...	0	7/2 ⁺	7/2 ⁺
0.130	1	52.5	0.31	0.129	p _{1/2}	75	1/2 ⁻	0.130	1/2 ⁻	1/2 ⁻
0.149 (D) ^c	4	29.5	0.87	0.150 (D)	{g _{9/2} (p)}	145	9/2 ⁺	0.149	9/2 ⁺	9/2 ⁺
0.393	1	17.5	0.10	0.401	p _{3/2}	65	(1/2 ⁻ , 3/2 ⁻)	...	3/2 ⁻	?
(0.410)	...	29	0.16	3/2 ⁻	0.393	3/2 ⁻	3/2 ⁻
(0.46)	...	weak
...	...	weak	0.456	3/2 ⁻	3/2 ⁻
0.498	2	20	0.11	0.474	g _{9/2}	6.5	9/2 ⁺	0.470	5/2 ⁺	5/2 ⁺ , 7/2 ⁺ , 9/2 ⁺ (D?)
(0.52)	...	poorly resolved	...	0.499	...	weak	3/2 ⁺ , 5/2 ⁺	0.499	(7/2, 9/2) ⁺	(5/2 ⁺)
...	0.524	...	50
0.723	2	9.9	0.05	0.639	7/2 ⁺	7/2 ⁺
0.762	2	21	0.11	0.783	p _{3/2}	125	3/2 ⁻ , 5/2 ⁺	0.724	5/2 ⁺	5/2 ⁺
...	3/2 ⁻ , 5/2 ⁺	0.762	3/2 ⁻	3/2 ⁻ , 5/2 ⁺
0.787	3 or (2)	39	(1.06)	0.786	3/2 ⁻	3/2 ⁻
0.807	(2)	37	(0.20)
...	0.806	3/2 ⁺	3/2 ⁺
(0.869) (D)	...	weak	...	0.817	(f _{5/2})	10	(3/2 ⁺ , 5/2 ⁺)
(0.899)	...	weak	...	0.858	p _{3/2}	20	(5/2 ⁻)
...	0.898	f _{7/2}	50	(3/2 ⁻)
...	0.924	...	weak	(7/2 ⁻)
0.969 (D)	(4)	24	(0.65)
(1.016)	(2)	21	(0.11)	(7/2, 9/2) ⁺	(7/2 ⁺ , 9/2 ⁺)
...	(3, 4)	10.5	(0.27)	(3/2 ⁺ , 5/2 ⁺)	0.970	5/2	5/2 ⁺
...	(1.062) (D)	...	weak
...	(1.126)	...	weak
...	1.190	(p _{3/2} , f _{7/2})	6	(3/2 ⁻ , 7/2 ⁻)
...
(1.320)	...	weak	1.215
...	(1.269)
...	1.321
...	(1.368)	...	weak	...	1.345
...
...	1.393	(g _{9/2} , f _{7/2})	10	(9/2 ⁺ , 7/2 ⁻)	1.377
...
1.487	2	18.5	0.1	(1.442)
...	or (3)	...	(0.43)	1.487	...	(3/2, 5/2)
...	1.521	f _{7/2}	15	7/2 ⁻
...	(1.543)	...	weak	(7/2 ⁻)
...	1.577	(g _{9/2} , f _{7/2})	4.5	(9/2 ⁺ , 7/2 ⁻)

TABLE III (Continued)

Ru ¹⁰⁴ (He ³ , d)Rh ¹⁰⁵		Pd ¹⁰⁸ (p, α)Rh ¹⁰⁵		β-γ decay ^b	
Excitation energy (MeV)	$\frac{d\sigma^a}{d\Omega}$ (μb/sr)	Excitation energy (MeV)	l_j	$(d\sigma/d\Omega)_{\max}$ (μb/sr)	Excitation energy (MeV)
	l	$(2I_{r+1})S$		J^π limits present work	J^π
...				...	1.698
1.719	3 or 2	(0.6 or 0.1)		(3/2 ⁺ , 5/2 ⁻)	1.720
1.762 (D)	2	0.11		3/2 ⁺ , 5/2 ⁺	...
(1.829)	(2 or 3)	(0.04 or 0.2)	
1.864	3 or 2	(0.82 or 0.17)		(5/2 ⁻)	...
1.913	2	0.04		3/2 ⁺ , 5/2 ⁺	...
1.957 (D)	3 or (2+4)	(0.61) (0.06, 0.38)		(5/2 ⁻)	...

^a Differential cross section near stripping peak (10° for $l=1$; 15° for $l=2$; 25° for $l=3$; 30° for $l=4$).

^b Ref. 8.

^c Means suggested doublet.

these levels are presented, but no definite spin and parity assignments are offered. The predicted $f_{5/2^+} - f_{7/2^+}$ j dependence is illustrated with the 0.524-MeV data.

IV. DISCUSSION OF LEVELS OF Rh¹⁰⁵

The early studies³⁻⁷ of the levels of Rh¹⁰⁵ involved radioactive decay of the 4.44-hr-half-life Ru¹⁰⁵ nucleus. Unfortunately, these results suffered from the inadequacy of scintillation-counter resolution, as well as an incorrect spin assumption for the parent nucleus made in many of these investigations. Recent γ - γ and β - γ decay work by Schriber and Johns⁸ removed many of the earlier inconsistencies, and represents the only high-resolution study of Rh¹⁰⁵ reported to date.

The $7/2^+$ ground state¹⁹ of Rh¹⁰⁵ has been described^{8,20} as a seniority-three ($g_{9/2}$)³_{7/2} proton configuration, and, as one would expect from orthogonality with the seniority-zero Ru¹⁰⁴ and Pd¹⁰⁸ target nuclei, it was excited only very weakly by the (He³, d) and (p, α) studies. In agreement with all previous decay work, the first excited 0.130-MeV (isomeric) level was populated by $l_p=1$ in the Ru¹⁰⁴(He³, d) data and verified as $1/2^-$ by the j -dependent $p_{1/2}$ (p, α) angular distribution (see Fig. 5).

On the basis of internal-conversion data and the absence of β feeding, $J^\pi = 9/2^+$ was assigned⁸ to the 0.149-MeV level. (He³, d) and (p, α) strongly excite this state by $g_{9/2}$ transfer; but the small-angle trend of both angular distributions differs from other $l=4$ transfers in a way that might be explained by an $l=1$ admixture. The excellent composite fit (Fig. 5) to the (p, α) data of good statistics, makes it tempting to postulate an unresolved $3/2^-$ or $1/2^-$ level very close to the $9/2^+$ state; however, the existing γ data offer little support for this suggestion. A 246-keV line which might be expected from the feeding of this new level by the established $3/2^-$ state at 0.393 MeV has been observed by Schriber and Johns,⁸ but γ - γ coincidence relationships require its placement elsewhere in the decay scheme. It is possible that the intense 0.393 → 0.129-MeV transition masks a weaker decay to the level near 0.149 MeV.

The 0.393-MeV state has been assigned⁸ $3/2^-$ on the basis of $M1$ decay to the 0.130-MeV level and coincidence measurements linking it to known higher levels. The $l=1$ transfer seen in the proton transfer is consistent with this designation, and the $p_{3/2}$ experimental (p, α) angular distribution confirms $3/2^-$. Nonlinearity effects experienced near the ends of the position counters are probably responsible for the slight discrepancy in excitation energy noted for the (p, α) determination.

In Rh¹⁰⁵ the stripping and pickup reactions gen-

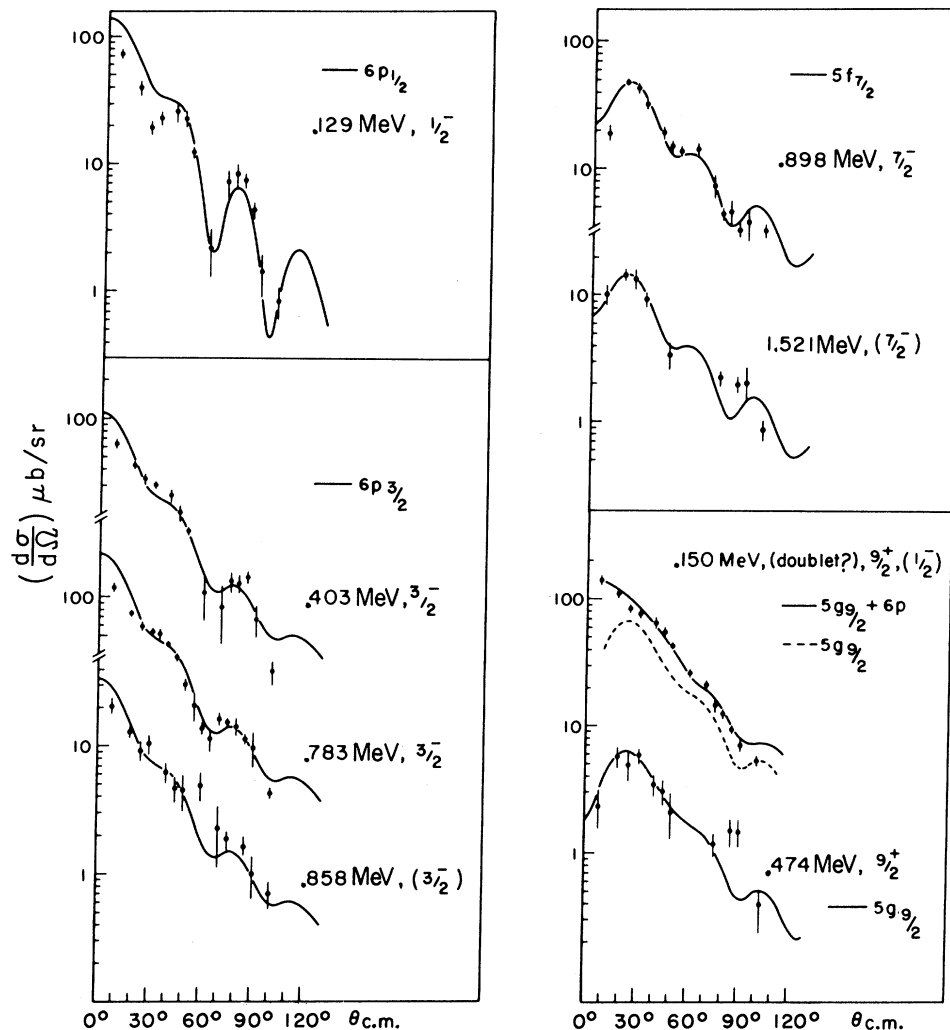


FIG. 5. Comparison of DWBA calculations with statistically significant angular distributions resulting from the $\text{Pd}^{108}(p, \alpha)$ investigation at $E_p = 15$ MeV. DWBA predictions duplicate quite well the measured $l=1$ j dependence.

erally populate different levels at higher excitations and, in many cases, states not excited by radioactive decay. The 456-keV level⁸ is not seen in (p, α) and only weakly in (He^3, d) . For the 0.469-MeV level, Schriber and Johns restrict J^π to $\frac{5}{2}^+$ through $\frac{11}{2}^+$, and choose a $\frac{5}{2}^+$ assignment on account of apparent $E1$ feeding from the $\frac{3}{2}^-$ 0.786-MeV state. However, the 0.470-MeV state is not excited by (He^3, d) , and d transfer is unlikely in $\text{Pd}^{108}(p, \alpha)$. The moderately weak 0.474-MeV (p, α) transition is best duplicated by $l=4$ ($g_{9/2}$) pickup calculations. Neeson and Arns,³ previously had suggested a $\frac{9}{2}^+$ assignment, although a re-interpretation of their analysis assuming the currently accepted $\frac{3}{2}^+$ Ru^{105} parent spin would also allow $\frac{7}{2}^+$ as a candidate. In view of the conflicting

information, it seems indicated to postulate a doublet with possible spins, ($\frac{5}{2}^+, \frac{7}{2}^+$) and $\frac{9}{2}^+$, respectively.

Internal-conversion measurements⁸ for the 0.499-MeV level limit spins to $\frac{5}{2}^+ \leq J^\pi \leq \frac{9}{2}^+$, although failure to detect β population of this level has led to a tentative ($\frac{7}{2}^+, \frac{9}{2}^+$) designation. Excited but weakly in (p, α) , this state is observed to be formed by $l=2$ transfer in (He^3, d) , and leads us to suggest a provisional $\frac{5}{2}^+$ spin and parity assignment instead.

The (p, α) data show a new and fairly strongly excited level at 0.524 MeV, but do not permit any definite l -transfer prediction. This level probably corresponds to the marginally resolved (0.52-MeV) state, weakly excited in the (He^3, d) reaction.

Levels near 0.724, 0.762, and 0.806 MeV are ex-

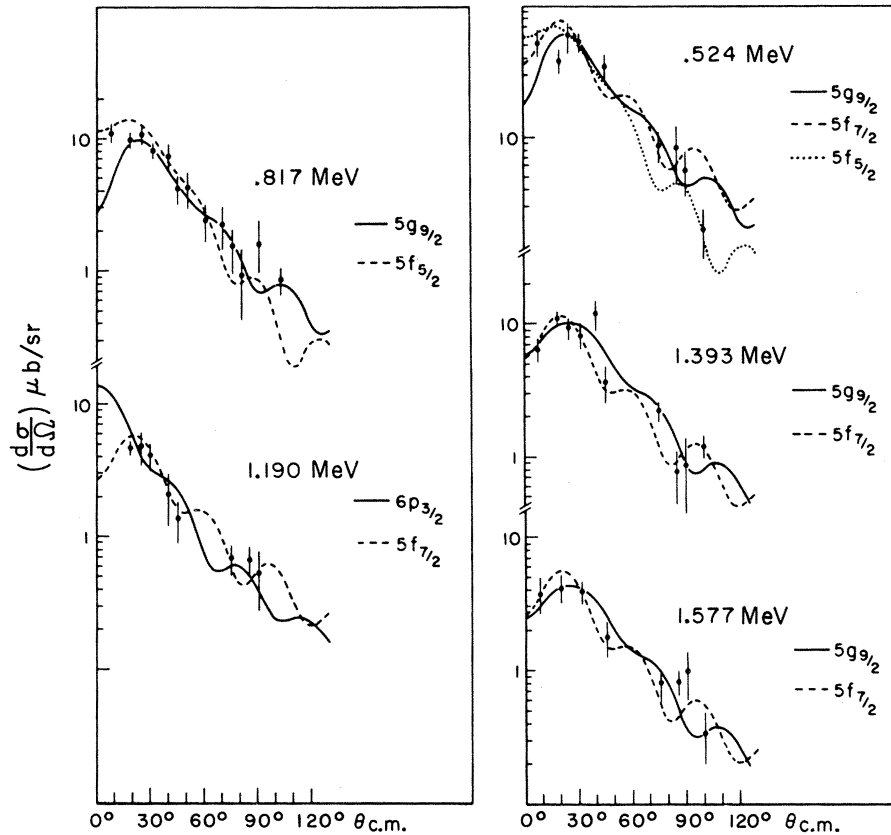


FIG. 6. Pd¹⁰⁸(p, α) transitions of less pronounced structure to more weakly excited levels in Rh¹⁰⁵. The calculated curves for $l=3$ and $l=4$ do not differ sufficiently to permit unique l assignments for data of poor statistics. Note that $f_{5/2}$ and $f_{7/2}$ angular distributions, shown with the 0.524-MeV level, are predicted to be measurably different.

cited by both radioactive decay and in (He^3, d). Deuteron angular distributions show an $l=2$ stripping pattern for all three; they corroborate the previous $5/2^+$ and $3/2^+$ assignments to the 0.724- and 0.806-MeV states, respectively, and restrict the unassigned 0.762-MeV state to $3/2^+$ or $5/2^+$. Failure to excite these states in (p, α) again reflects the inhibition of $l=2$ pickup expected on shell-model grounds.

A state in the vicinity of 0.785-MeV excitation has been included in most decay schemes,³⁻⁸ but little agreement exists as to its J^π assignment. The work of Schriber and Johns⁸ yields a $3/2^-$ designation for this level, while Neeson and Arns³ propose a spin and parity of $5/2^+$, $7/2^+$. The (p, α) angular distribution for this state, the second most strongly excited level [$d\sigma/d\Omega_{\text{max}} \approx 125 \mu\text{b/sr}$] observed in Pd¹⁰⁸, is well represented by a $p_{3/2}$ calculation (see Fig. 5) and supports the $3/2^-$ assignment. However, the (He^3, d) data clearly do not show the 20° minimum characteristic of $l=1$ transfer, and seem to reflect an $l=2$ or $l=3$ pattern. It

is suggested that we see a close doublet of levels with spins $3/2^-$ and $(5/2^-)$.

A fairly strong level is seen at 0.817 MeV in the (p, α) reaction, but not in any of the other reactions. $J^\pi = (5/2^-)$ is a likely assignment. Excitations identified in the pickup at 0.898 MeV and near 0.858 MeV are well reproduced (particularly the former) by $f_{7/2}$ and $p_{3/2}$ DWBA (p, α) predictions, respectively. Both levels are excited only weakly by the (He^3, d) experiment and are unobserved in Ru¹⁰⁵ decay.

β - γ and γ - γ studies⁸ establish a $5/2^+$ level at 0.970 MeV. The (He^3, d) energy spectra display a strong, broadened group at 0.969 MeV, suggestive of excitation of a multiplet of levels. The resulting stripping angular distribution for this group is rather structureless (see Fig. 4) and might be described by an $l=4+2$ calculation; an $l=3$ prediction is also drawn through the data and indicates the ambiguity involved in assigning an l transfer in this instance. On the basis of the previous well-authenticated β -decay assignment and the experi-

mentally observed level broadening in (He^3, d), a $\frac{5}{2}^+$ and ($\frac{7}{2}^+, \frac{9}{2}^+$) doublet is included in the Rh^{105} level scheme at this excitation. A $\frac{5}{2}^-$ assignment to one of the multiplet levels appears unlikely, as it is not excited in (p, α).

Only three states above 1 MeV proposed in decay work have been confirmed, as to excitation energy, by one or the other of our transfer studies. The 1.487-MeV level, unassigned by β -decay measurements,⁸ is limited to $\frac{3}{2} \leq J \leq \frac{5}{2}$ on the strength of the deuteron angular distribution. Based only on weak β decay in coincidence with a ground-state γ transition, a state at 1.720 MeV has been placed in the Rh^{105} scheme and assigned positive parity.⁸ (He^3, d) excites this level with a d - or f -stripping pattern. A level weakly populated in proton stripping at 1.321 MeV is also included in the level scheme of Schriber and Johns,⁸ but no suggestions for spin and parity can be made. Levels observed by only one of the modes of excitation are also listed in Table III together with their J^π limits when warranted by the data. However, poor statistics or lack of resolution often make definite l assignments difficult. (See Figs. 4 and 6.) In particular, the distinction between $l=2$ and $l=3$ in (He^3, d) is difficult unless statistics are good.

V. CONCLUSIONS

It has been found that the Rh^{105} spectrum is even more complex than previously suggested by Schriber and Johns. At least 20 new levels have been observed, which brings the total of established Rh^{105} states below 2-MeV excitation to over 40. Many levels excited by β - γ decay were not seen in the direct transfer reactions studied, and vice versa. The very selective population of these states should eventually lead to valuable restrictions for their wave functions, although initially this fact tends to complicate our attempt to establish reliable J^π assignments.

The high level density as well as limitations in statistics and resolution did not permit a systematic study of levels above 2 MeV. Hence we only have limits for the fullness or emptiness (U_j^2) of various proton single-particle states. No $l=2$ pickup was seen in (p, α). For Ru^{104} we find that the $2p_{1/2}$ state is at least 16% empty, and that the emptiness of the $2p_{3/2}$ state is $U_{p_{3/2}}^2 \geq 0.04$. For $1g_{9/2}$ we find $U_{g_{9/2}}^2 \geq 0.1$. There are good indications that the $1f_{5/2}$ state is partially empty; however, the difficulty of uniquely distinguishing between

$l=2$ and $l=3$ does not permit us to quote a definite number.

As might have been expected from the anomalous $\frac{7}{2}^+$ ground state of Rh^{105} , there is no simple model for the low-lying levels. While certain aspects of a weak-coupling model seem to apply, a detailed description of the observed level scheme in terms of the collective model is difficult. In analogy with the vibrational behavior of low-lying states for other nuclei in this mass region, one might expect a level ordering arising from the coupling of the collective excitations of the Ru^{104} core to the odd proton. Applying the single-particle-core weak-coupling model of de-Shalit,²¹ Ford *et al.*²² were able to describe the low excitations of Ag^{107} as a coupling of the odd $p_{1/2}$ proton to the one and two-phonon vibrations of the Pd^{106} core.

At low excitations in Rh^{105} , one might expect a multiplet with spins of $\frac{5}{2}^+$ to $\frac{13}{2}^+$ resulting from coupling of a $g_{9/2}$ proton to the 2^+ one-phonon core, as well as $\frac{1}{2}^-$ and $\frac{9}{2}^+$ levels from the 0^+ core + $g_{9/2}$ or $p_{1/2}$ configurations. In the vicinity of 1 MeV a set of 15 levels might be anticipated, arising from coupling of members of the two-phonon-core triplet to the $g_{9/2}$ particle. In addition, core vibrations might similarly be coupling to other proton configurations, further complicating the low-lying spectrum. Most positive-parity states identified in this region could result from this core + $g_{9/2}$ model. Observed levels of negative parity may well belong to collective multiplets arising from a coupling of the core states to a $p_{1/2}$ proton.

The DWBA analysis of $\text{Pd}^{108}(p, \alpha)$ angular distributions has given further good examples of the $l=1$ j dependence in the Pd region. There is also evidence for j dependence at larger l transfers (Figs. 5 and 6) in the sense that $f_{5/2}$ - $f_{7/2}$ DWBA predictions differ markedly, while the chosen curves show very good agreement with experiment. Further studies of this effect would be of great interest.

VI. ACKNOWLEDGMENTS

Assistance in the (p, α) data taking by Y. S. Park and J. Orloff was greatly appreciated. We are grateful for aid in development of a He^3 beam of usable magnitude by Dr. J. N. McGruer, R. Gibson, and M. Schneider. One of us (D.L.D.) would like to acknowledge valuable discussions with Dr. M. B. Lewis.

- *Supported by the National Science Foundation.
 †Present address: Analytic Services Inc., Falls Church, Virginia.
- ¹D. L. Dittmer and W. W. Daehnick, Phys. Rev. **187**, 1553 (1969); and Phys. Rev. **188**, 1881 (1969).
- ²See, for instance, R. O. Ginaven, A. M. Bernstein, R. M. Drisko, and J. B. McGrory, Phys. Letters **25B**, 206 (1967).
- ³J. F. Neeson and R. G. Arns, Nucl. Phys. **68**, 401 (1965).
- ⁴B. Saraf, P. Harihar, and R. Jambunathan, Phys. Rev. **118**, 1289 (1960).
- ⁵R. A. Ricci, S. Monaro, and R. Van Lieshout, Nucl. Phys. **16**, 339 (1960).
- ⁶H. W. Brandhorst, Jr., and J. W. Cobble, Phys. Rev. **125**, 1323 (1962).
- ⁷A. P. Arya, Nucl. Phys. **40**, 387 (1963).
- ⁸S. O. Schriber and M. W. Johns, Nucl. Phys. **A96**, 337 (1967).
- ⁹Nuclear Diodes, Inc., Prairie View, Illinois.
- ¹⁰J. B. Moorhead, Ph. D. thesis, University of Pittsburgh, 1969 (unpublished).
- ¹¹W. W. Daehnick, Phys. Rev. **177**, 1763 (1969).
- ¹²P. D. Kunz, University of Colorado DWBA code DWUCK, 1967 (unpublished).
- ¹³D. E. Rundquist, M. K. Brussel, and A. I. Yavin, Phys. Rev. **168**, 1287 (1968).
- ¹⁴W. C. Parkinson, D. L. Hendrie, H. H. Duhm, J. Mahoney, J. Saudinos, and G. R. Satchler, Phys. Rev. **178**, 1976 (1969).
- ¹⁵R. H. Bassel, Phys. Rev. **149**, 791 (1966).
- ¹⁶S. Yoshida, Nucl. Phys. **38**, 380 (1962).
- ¹⁷F. G. Perey, Phys. Rev. **131**, 745 (1963).
- ¹⁸W. B. Cheston and A. E. Glassgold, Phys. Rev. **106**, 1215 (1957).
- ¹⁹W. R. Pierson, Phys. Rev. **140**, 1516 (1965).
- ²⁰M. G. Mayer and J. H. D. Jensen, *Elementary Theory of Nuclear Shell Structure*, (John Wiley & Sons, Inc., New York, 1955).
- ²¹A. de-Shalit, Phys. Rev. **122**, 1530 (1961).
- ²²J. L. C. Ford, Jr., C. Y. Wong, T. Tamura, R. L. Robinson, and P. H. Stelson, Phys. Rev. **158**, 1194 (1967).

Study of the Energy Levels of ²⁰³Tl Using (γ, γ') Reaction

R. Moreh, A. Nof, and A. Wolf

Nuclear Research Centre-Negev, Beer Sheva, Israel

(Received 12 March 1970)

Elastic and inelastic nuclear resonant scattering of monochromatic photons from ²⁰³Tl has been studied using a 20-cc Ge(Li) detector. The γ source was obtained from thermal-neutron capture in titanium. The scattering isotope was identified by using an isotopically enriched thallium target. The energy of the resonance level in ²⁰³Tl was found to be 6.418 MeV. Assuming the high-energy lines to be primary transitions deexciting the resonance level, some 14 energy levels were found from the ground state up to 2.9 MeV, 4 of which may be identified with recently reported levels.

By measuring the angular distribution of the scattered radiation, the spin of the 6.418-MeV level was determined to be $\frac{1}{2}$, and thus, based on the assumption of dipole transitions, the spins of several low-lying levels were found to be either $\frac{1}{2}$ or $\frac{3}{2}$. The total radiative width of the resonance level was determined and found to be $\Gamma_\gamma = 0.32 \pm 0.06$ eV and $\Gamma_0/\Gamma_\gamma = 0.026$. The spectral shape of scattered radiation was found to have a strong intensity bump at about 5 MeV; this is discussed in the light of similar bumps obtained in (n, γ) and ($d, p\gamma$) reactions on nuclei in the same mass region.

I. INTRODUCTION

The use of the (γ, γ') reaction for studying the properties of excited nuclear levels is by now a well-known technique.^{1,2} In the present work, monochromatic photons obtained from thermal-neutron capture in titanium were used as a γ source; the elastic and inelastic scattered γ radiation from a Tl target³ was studied using a Ge(Li) detector. The scattering isotope was identified by using an enriched target. The total radiation width of the 6.418-MeV resonance level was measured by means of an absolute cross-section measure-

ment, a self-absorption experiment, and a temperature-variation experiment. From an angular-distribution experiment, information was obtained about the spin of the resonance and low-lying levels, and a level scheme for ²⁰³Tl is presented. An anomalous intensity bump was observed in the scattered radiation spectrum of ²⁰³Tl, as was the case in the scattered radiation spectrum^{1,4} of ²⁰⁵Tl. The low-energy levels in ²⁰³Tl are discussed in terms of recent theoretical calculations.

II. EXPERIMENTAL PROCEDURE

A thermal-neutron flux was provided by the Is-